

Performance optimization and analysis of the unstructured discontinuous Galerkin solver on multi-core and many-core architectures

1st Zhe Dai

*Computational Aerodynamics Institute
China Aerodynamics Research and Development Center
Mianyang, China
daizhe_cardc@163.com*

2nd Liang Deng*

*Computational Aerodynamics Institute
China Aerodynamics Research and Development Center
Mianyang, China
dengliang11@nudt.edu.cn*

3rd Yueqing Wang

*Computational Aerodynamics Institute
China Aerodynamics Research and Development Center
Mianyang, China
yqwang2013@163.com*

4th FangWang

*State Key Laboratory of Aerodynamics
China Aerodynamics Research and Development Center
Mianyang, China
wangfang@cardc.cn*

5th Ming Li

*Computational Aerodynamics Institute
China Aerodynamics Research and Development Center
Mianyang, China
liming@cardc.cn*

6th Jian Zhang

*Computational Aerodynamics Institute
China Aerodynamics Research and Development Center
Mianyang, China
zhangjian@cardc.cn*

Abstract—The discontinuous Galerkin (DG) algorithm is a representative high order method in Computational Fluid Dynamics (CFD) area which possesses considerable mathematical advantages such as high resolution, low dissipation, and dispersion. However, DG is rather computationally intensive to demonstrate practical engineering problems. This paper discusses the implementation of our in-house practical DG application in three different programming models, as well as some optimization techniques, including grid renumbering and mixed precision to maximize the performance improvements in a single node system. The experiment on CPU and GPU shows that our CUDA, OpenACC, and OpenMP-based code obtains a maximum speedup of 42.9x, 35.3x, and 8.1x compared with serial execution by the original application, respectively. Besides, we systematically compare the programming models in two aspects: performance and productivity. Our empirical conclusions facilitate the programmers to select the right platform with a suitable programming model according to their target applications.

Index Terms—Unstructured grid, DG, GPU, performance, productivity

I. INTRODUCTION

The high-order scheme receives considerable attention in Computational Fluid Dynamics (CFD) due to its low numerical dissipation for Large-Eddy Simulation (LES) [1] and the capability to capture the fine-grained structure in complicated flows. Discontinuous Galerkin (DG) [2] is a popular

algorithm that possesses good mathematical properties in conservation, stability, and convergence in complex flow problems. However, DG suffers from severe computing overhead comparing with the low-order scheme. For example, solving the Euler equation with three-dimensional fourth-order DG method needs one hundred variables per grid element [3], [4], while the only single-digit variable is required in low-order methods, not to mention the additional volume and area integral computations in every grid element, which is not needed at all in low-order method.

To make computationally expensive DG algorithm available in practical engineering, many researchers have made considerable achievements on both GPU and CPU hardware. Xia accomplishes the unstructured grid DG algorithm based on OpenACC Programming model [5]. Pazner employed a parallel-in-time strategy to compute the Runge-Kutta stages simultaneously under DG discretizations [6]. Duan applied total variation diminishing Runge-Kutta scheme coupled with the multigrid strategy to improve the parallel efficiency of DG method on CPUs [7]. Maurice presented a parallel computing strategy for a hybridizable discontinuous Galerkin nested geometric multigrid solver on many-core hardware, attaining 80% of peak performance for higher order polynomials [8]. Kronbichler integrated optimized DG code into a scalable framework of five supercomputers using both CPU and GPU hardware [9].

The former studies usually focus on the algorithm optimization

*Corresponding author: dengliang11@nudt.edu.cn. This work was supported by the National Numerical Wind Tunnel of China.

tion and performance achievement with either CPU or GPU. However, few articles consider the performance portability across multi-core CPU and many-core accelerators, as they are generally used in high performance computing (HPC) system. The latest TOP500 list shows that six out of the top ten supercomputers utilize many-core accelerators, this trend brings not only a good opportunity to accelerate DG algorithm on GPU, but also barriers in programming to migrate code on diverse computing architectures.

Therefore, this work aims to assess three programming models, namely OpenMP, OpenACC, and CUDA on both multi-core CPU and many-core accelerator, in the context of an unstructured grid high-order DG application called HOUR2D. The aspects to be compared are the implementation effort and performance evaluation, as well as the optimizations during code migration. Finally, we evaluate the performance and portability to give insights on appropriate language selection for different purposes. The work provides novelty from several perspectives:

- We give a high-performance migration of HOUR2D application in OpenMP, OpenACC, and CUDA, respectively, the parallelization in different programming models is elaborately chosen to adapt unique data structures and computing formats.
- We perform the grid renumbering method to optimize irregular memory access issue caused by the unstructured grid, then carry out the mixed floating-point method to improve computational performance, at last, the Unified Memory(UM) method are tested in OpenACC for workload reduction.
- We evaluate the performance and productivity, firstly the speedup of three programming models is listed using six different grid meshes, then some insights are indicated by using the roofline model, at last, a comprehensive assessment is displayed together with productivity metric.

This work is organized as follows: Section 2 gives a brief review of the mathematical method and typical data pattern used in HOUR2D. Section 3 displays the implementation to achieve high performance for three programming languages and the evaluation approaches. Section 4 presents the experiment of performance and productivity in HOUR2D code. Section 5 summarizes our whole research and gives insights.

II. HOUR2D MATHEMATICAL METHOD

HOUR2D can solve steady or unsteady field Navier-Stoke and Euler problems by using the explicit Runge-Kutta high-order DG algorithm, and it's mainly composed of three parts: preprocessing, flow field calculation, and output postprocessing. The application uses the same high-order DG numerical method to discretize the Euler equation and Navier-Stokes equation, the governing equation, and the detailed numerical discretization process are as follows.

A. Governing Equation

In the Cartesian coordinate system, the two-dimensional conserved form Navier-Stokes or Euler equations without

regard to volume force and external heating are:

$$\frac{\partial Q}{\partial t} + \frac{\partial E}{\partial x} + \frac{\partial F}{\partial y} = ivis \cdot \left(\frac{\partial E_v}{\partial x} + \frac{\partial F_v}{\partial y} \right) \quad (1)$$

where Q is conserved variable, while $(E, F)/(E_v, F_v)$ are inviscid/viscous flux in x, y direction respectively, eq. (1) is Euler equation when $ivis = 0$, otherwise is NS equation when $ivis = 1$. The detailed formation is

$$Q = \begin{bmatrix} \rho \\ \rho\mu \\ \rho\nu \\ e \end{bmatrix}, E = \begin{bmatrix} \rho\mu \\ \rho\mu^2 + p \\ \rho\mu\nu \\ (e+p)\mu \end{bmatrix}, F = \begin{bmatrix} \rho\nu \\ \rho\nu\mu \\ \rho\nu^2 + p \\ (e+p)\nu \end{bmatrix} \quad (2)$$

$$E_\nu = \begin{bmatrix} 0 \\ \tau_{xx} \\ \tau_{xy} \\ \mu\tau_{xx} + \nu\tau_{xy} - q_x \end{bmatrix}, F_\nu = \begin{bmatrix} 0 \\ \tau_{yx} \\ \tau_{yy} \\ \mu\tau_{yx} + \nu\tau_{yy} - q_y \end{bmatrix} \quad (3)$$

where ρ is the density, and μ, ν is the velocity in x, y direction, p is the pressure, and e is total fluid energy per unit volume written as:

$$e = \rho \left[U + \frac{1}{2}(\mu^2 + \nu^2) \right] = \frac{p}{\gamma - 1} + \frac{1}{2}\rho(\mu^2 + \nu^2) \quad (4)$$

while U is the internal energy per unit mass of fluid:

$$U = C_v T = RT / (\gamma - 1) = p / \rho / (\gamma - 1) \quad (5)$$

where $C_v = R / (\gamma - 1)$ is specific heat capacity at constant volume, T is the temperature obtained from state equation $p = \rho RT$, R is gas constant, γ is specific heat ratio. $\tau_{xx}, \tau_{xy}, \tau_{yx}, \tau_{yy}$ are the weights of viscous stress tensor, Stokes' hypothesis for a Newtonian, isotropic fluid can be written as:

$$\tau = \begin{bmatrix} \tau_{xx} & \tau_{xy} \\ \tau_{yx} & \tau_{yy} \end{bmatrix} = \mu \begin{bmatrix} 2/3(2\mu_x - \nu_y) & \mu_y + \mu_x \\ \mu_y + \mu_x & 2/3(2\nu_y - \nu_x) \end{bmatrix} \quad (6)$$

where ν is dynamic viscosity coefficient.

B. DG Discretization

The governing equation in eq. (1) can be abbreviated as

$$Q_t + \nabla \cdot \vec{F}(Q) - \nabla \cdot \vec{F}_\nu(Q, \nabla Q) = 0 \quad (7)$$

compared with the second-order finite volume (FVM) discretization method, all the physical quantities of every element obey high-order polynomial distribution in DG discretization way, which means the corresponding distribution polynomial coefficients are needed, scilicet, degrees of freedom.

$$Q(t, x, y) = \sum_j c_j(t) b_j(x, y) \quad (8)$$

c_j in eq. (8) is the physical quantity coefficient in element which varies over time, b_j is basis function, then introducing auxiliary variables based on eq. (8):

$$Q_t + \nabla \cdot \vec{F}(Q) - \nabla \cdot \vec{F}_v(Q, \vec{Z}) = 0 \quad (9)$$

afterward multiplying again by basis function b_j , at last, we get a discrete form of the discontinuous finite element using integration by parts :

$$\begin{aligned} & \int_{\Omega} \vec{Z} b_j d\Omega = \\ & - \int_{\Omega} Q \cdot \nabla b_j d\Omega + \int_i \hat{Q}(Q^-, Q^+) \vec{n} b_j d\Gamma \\ & + \int_b \hat{Q}^b(Q^-, Q^b) \vec{n} b_j d\Gamma \int_{\Omega} Q_t b_j d\Omega \\ & - \int_{\Omega} (\vec{F}(Q) - \vec{F}_v(Q, \vec{Z})) \cdot \nabla b_j d\Omega \\ & + \int_i \vec{H}_c(Q^-, Q^+, \vec{n}) b_j d\Gamma \\ & + \int_b \vec{H}_c^b(Q^-, Q^b, \vec{n}) b_j d\Gamma \\ & - \int_i \vec{H}_v(Q^-, \vec{Z}^-, Q^+, \vec{Z}^+, \vec{n}) b_j d\Gamma \\ & - \int_b \vec{H}_v^b(Q^-, \vec{Z}^-, Q^b, \vec{Z}^b, \vec{n}) b_j d\Gamma \\ & = 0 \end{aligned} \quad (10)$$

The spatial integral in eq. (10) is a Gaussian Numerical Integral of which the subscripts Ω, i, b represents the element integral, the interior surface integral, and the boundary surface integral respectively, while the superscript $-, +, b$ represents the physical quantity inside the element, outside the element, and at the boundary conditions. H_c denotes inviscid flux which is in Roe format [10], besides H_v is viscous flux in BR1 format [11].

III. PERFORMANCE IMPLEMENTATION

Time iterations is the hotspot which occupies more than 95% of total running time which is shown detailedly in fig. 1, including time step, right-hand-side(RHS), and file output, the RHS procedure involves inviscid flux, gradient, viscous flux, and residual calculation. The RHS step is counted twice in every time step because of the two-order explicit Runge-Kutta method, and it consumes approximately 90% of total running time, so it is the computationally intensive part of the whole application indeed, therefore the primary concern for performance optimization is RHS.

A. Data Structure and Computing Formats

The geometric topology of HOUR2D's unstructured mesh consists of vertices, elements, and cells as shown in fig. 2, E_i is the face unit in which stores the flux variable, C_i is the cell unit in which stores the intermediate variables that include density, velocity, and pressure, besides the above data is organized as the array of structure(AOS) format.

We display two major computational modes that affect memory access pattern and parallelization format as the dotted

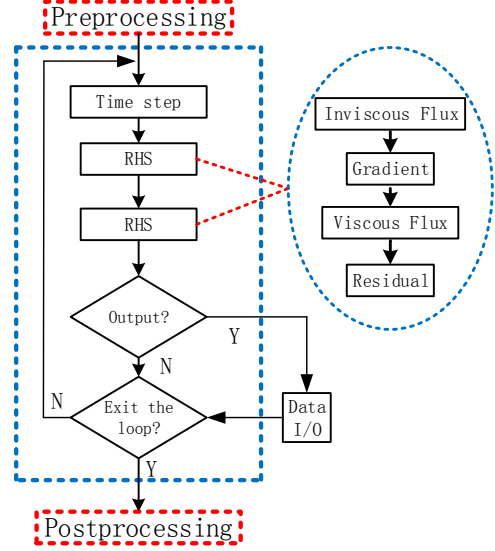


Fig. 1. The major work flows for HOUR2D application.

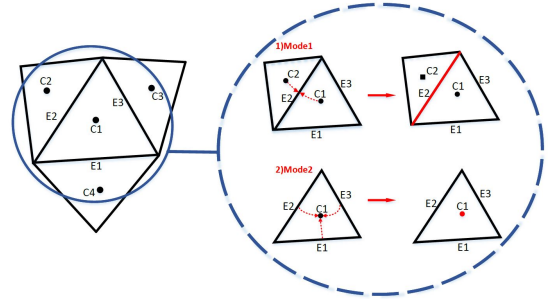


Fig. 2. Data structure and major computational modes. C is the body center of the cell, and E is the face unit where the data is stored in AOS format. The dotted box shows two major modes in our computations, the red dotted arrow means the data access flows in memory.

box shows. The first one indicates the flux computation which is parallelized through elements, for every time step, the program reads the intermediate variables from neighbor cell units, then writes back to the current element unit after calculations. The other one is the physical quantity calculations that are stored in cells, which requires flux variable around adjacent cells at the present step, data race occurs if the element parallelization model is still utilized.

B. Grid Renumbering

The second computing formats mentioned in the former subsection involves the data access around the neighbor cells in every central cell. However, the number of these adjacent cells are not naturally continuous as the topology of unstructured grid is irregular. Hence, resulting in indirect memory access patterns when iterating over the cells of the unstructured grid for the flux, gradient, and residual computations.

To relieve the irregular memory access issue, we reorder the grid to reduce the cache miss and improve the data

locality with Reverse Cuthill Mckee (RCMK) algorithm [12]. The RCMK is developed to minimize the bandwidth in the adjacent graph by assembling the non-zero values as close as possible to the main diagonal [13]. So we reorder the topological adjacency derived from the computational grid to align the cell numbers. The optimization result is shown in table I, it displays the bandwidth of four unstructured grids with different number of cells. The last two columns are the bandwidth of cell-based adjacency matrix which shows the degree of aggregation around the diagonal, the bandwidth is greatly reduced according to the results of all four grids, it can be inferred that bandwidth reduction obtains 2-3 orders of magnitude. A more detailed plot about the cell aggregation is shown in fig. 3, it exhibits the fairly good result by comparing the adjacency before and after applying RCMK.

TABLE I

THE BANDWIDTH OF DIFFERENT COMPUTATIONAL GRIDS WHEN USING RCMK ALGORITHM. THE ELEMENT IS THE NUMBER OF GRID CELLS, BANDWIDTH SHOWS THE MAX AGGREGATION OF ADJACENT ELEMENTS, THE BANDWIDTH IS GREATLY REDUCED AFTER APPLYING RCMK.

Grids	Number of cell	Original bandwidth	RCMK bandwidth
Grid1	2688	1427	69
Grid2	4032	3992	35
Grid3	16128	12410	67
Grid4	64512	49016	131

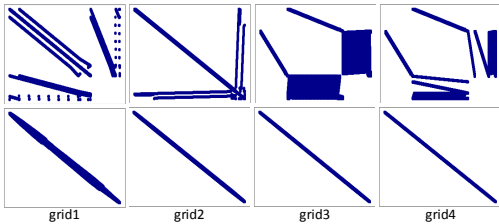


Fig. 3. The intuitive illustration for bandwidth reductions of four computational grids. The upper figures show the original adjacency, while the lower figures are adjacency after applying RCMK.

Following the renumbering, the cell is arranged in the order of monotonical index, and a consecutive rank is performed on the element index according to the first constant cell index, so the second index reference will be visited in ascending order. The staple benefits of the optimizations above can be summarized as enhancing both spatial and temporal locality particularly when cells are referenced contiguously in memory and exploiting the available memory bandwidth. What's more, the renumbering technique is executed only once before the time iteration starts for every process, hence it has a negligible effect on the whole application execution not to mention the time iteration is usually a fairly big number. The overall performance improvement by using the grid renumbering method is about 20%-30%.

C. Mixed Precision

The physical variables use the double-precision (DP) format to maintain good convergence and computational precision through CFD simulations compared with single-precision (SP), however, it increases the amount of memory data required for every floating-point operation, and the memory wall issue is further aggravated and restricts the CFD performance efficiency, under the conditions that off-chip memory bandwidth is considered to be the constraining resource in system performance for the foreseeable future [14]. The mathematical evidence proves that there's no need to use DP format in the all physical parameters or the whole calculation procedures, even if taking into account the constraint of given computational precision [15], [16], so CFD application turn to use lower floating-point precision variables to achieve higher performance, naturally some mixed-precision(MP) strategies emerged [17], [18].

One of the methods is called the iterative refinement approach, at first, it employs SP parameters in previous iterations to improve the computational performance, then uses DP format immediately when the convergence rebound occurs, so convergence, precision, and high performance are guaranteed at the same time. We verify this approach in HOUR2D by using a NACA airfoil mesh grid as the fig. 4 shows, fig. 4 illustrates the L_2 residual convergence, in which MP-30k stands for the initial 30 thousand steps are computed in SP format, while the rest of the steps are computed in DP, it's obvious that the precision of the output result decline as the SP step increases.

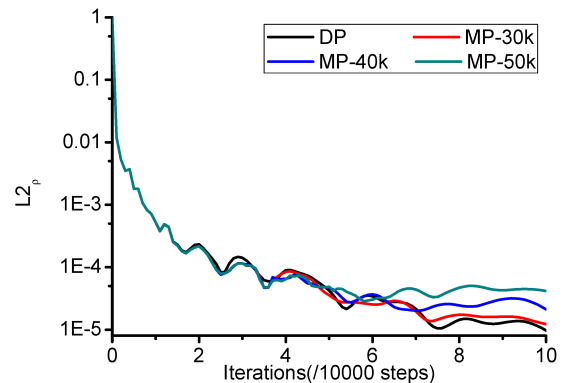


Fig. 4. Mixed precision approach verification using NACA grid. The comparison of the residual convergence in MP methodology with different time steps allocated in SP and DP, for example, MP-30k means the initial 30000 iterations are executed in SP format, the rest of the iterations are computed in DP.

We assess the performance improvement of our MP method after the correctness verification with two grid examples as table I shows. The experiment result is shown in table II, in which the total time steps are 100 thousand, too. DP shows the benchmark of our test, the run time decreases as the SP step increases. The last row SP indicates the most optimal improvement with no DP format variables are used at all, we can conclude from the table that the MP method achieves

15% performance improvement at most compared with the DP format. However, the SP format is only comparable in performance, as the computational precision is not strictly guaranteed to meet the constraint in diverse grids from mathematical point of view, the SP format are usually not used in engineering computations, so the most optimal speedup is usually only a theoretical conclusion.

TABLE II

CLOCK TIME OF OUR MIXED PRECISION APPROACH RUNNING ON TWO GRIDS. THE DP MEANS THE DOUBLE PRECISION CALCULATION, AND SP IS SINGLE PRECISION FORMAT, THE MP-20K MEANS THE STARTING 20000 ITERATIONS ARE EXECUTED IN SP FORMAT, FOLLOWED BY THE REST OF THE ITERATIONS COMPUTED IN DP.

Time	Grid1	Grid2
DP	51.87	151.91
MP-20k	49.68	145.83
MP-50k	48.30	140.90
MP-80k	46.68	135.95
SP	43.87	131.40

D. Heterogeneous Implementations

We port HOUR2D code using both Compute Unified Device Architecture(CUDA) and OpenACC on Nvidia GPU to get an apparent comparison in performance and productivity. CUDA usually gains a better performance than OpenACC due to the fine-grained manipulation of hardware resources within kernels, however, this generally requires the time-consuming task of code revising to make use of the resources for developers. On the contrary, OpenACC is a declarative model using compiler pragmas which is not as effective as CUDA in computing performance.

The minimization of data transmission between CPU and GPU hardware is at prior consideration in HOUR2D as it's an expensive operation over the time iterations, so the covered data is transported to GPU memory in the grid initialization stage to avoid the potential bottleneck caused by the frequent data transfer. We accommodate the grid data with the appropriate component from the GPU memory hierarchy like shared memory, constant memory, and global memory to achieve better memory access performance. For example, HOUR2D high-order algorithm needs 393 geometrical constants to accomplish element-integral and cell-integral in each time iteration step, so we place it in the constant memory to reduce memory transactions launched by thread warp.

As for the code migration, we port the whole iteration code into GPU as the blue dotted box shows in fig. 1, on the one hand, the parallelization in *RHS* step can be implemented naturally in the way of fig. 2 shows without any data racing, the element-based or cell-based loop can be mapped to the one-dimensional thread in GPU directly.

On the other hand, the time step computation involves the minimal value of all local time steps in cell data, making data racing if it's executed in direct parallelization. To achieve effective performance in entire computing procedures, we use GPU reduction to get minimal value by taking advantage of

shared memory which enables synchronization within thread blocks. Furthermore, we design the consecutive reduction method to realize robust reduction under the restriction of max thread number in GPU block.

Porting the code by using OpenACC is much more convenient than CUDA by using compiler pragmas to parallelize compute-intensive code, for example, the time step reduction mentioned above only needs to use `#pragma acc parallel reduction` instead, and the specified process will be done by PGI compiler, but the performance also highly depends on the data layout in PGI compiler and the effectiveness of code generation.

UM is a pragmatic technology that can be used by CUDA 6.X or higher version, it manages the data between CPU and GPU independently which was relied on programmers, hence explicit function calls and data migration can be decreased evidently. We adopt the UM method during heterogeneous code migration by simply adding the *managed* compilation option so that memory space between host and device is established.

UM leads to possible performance loss due to the additional memory transmission and memory page fault [19], which is also observed in our OpenACC code, generally, the performance loss decreases as the grid size increases, eventually stabilizing below 3% especially when the grid's element exceeds sixteen thousand, this may be caused the intensification of discontinuous memory access as grid size increases.

IV. EXPERIMENTS AND ANALYSIS

The HOUR2D code is fulfilled at the same level of optimization in three different programming models: OpenMP, OpenACC, and CUDA, while the computing hardware includes a computing node consisting of an Intel Xeon E5-2698 @2.20GHz CPU and an Nvidia A100 GPU, as for compiler toolchain, we use *GCC* - 5.4.0 for CPU code with optimization flag `-O3`, and the GPU compiler *NVCC* - 10.2.89 for CUDA and OpenACC. The computational grid is illustrated in table III which includes two steady NACA airfoil grids(grid1 and grid2), four unsteady front step grids (grid3-grid6), and an unsteady flow around double cylindrical(grid7). The latter grid is four times larger than the former one for those possess same aerodynamic shape, the last column is the grid type of every element.

A. Evaluation Approach

As the main hotspot of HOUR2D is time iteration that performs almost the same operation, and tens of thousands of time steps are usually required to reach a convergent result in practical CFD simulation, the preprocessing and postprocessing parts should be removed for the seek precise evaluation. We apply Dual-phase measurement [20] method to exclude the non-primary impacts during the performance experiments. Specifically, the application is tested twice with different iterations, the subtraction data between two iterations shows the difference of exact iteration computations. Hence,

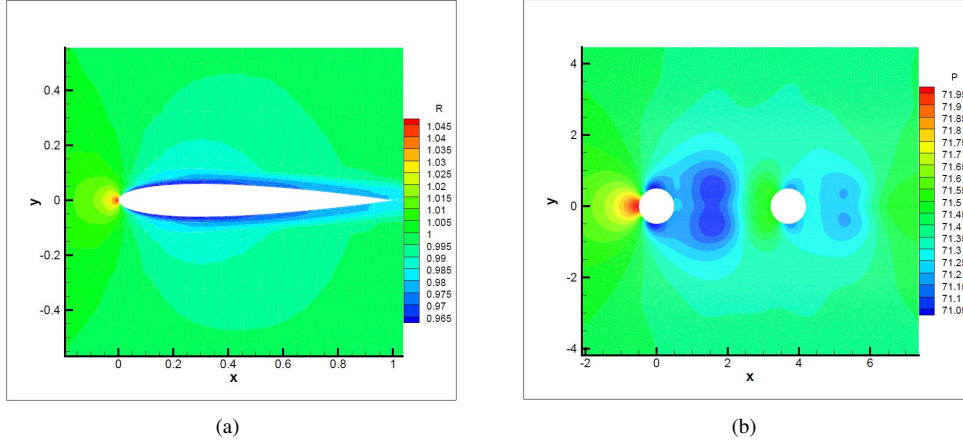


Fig. 5. Streamline diagram of the real computing results. (a) The density of grid2, with Mach number=0.3, Reynolds number=5000 at 400 thousand time steps. (b) The pressure of double cylindrical, with Mach number=0.1, Reynolds number=100 at 400 thousand time steps.

TABLE III

DETAILED INFORMATION OF COMPUTATIONAL GRIDS USED IN SUBSEQUENT EXPERIMENTS. NODES AND CELLS SHOW THE COMPUTATIONAL SCALE, THE DIFFERENCE OF GRID SHAPE REFLECTS THE NUMBER OF FACES IN CELL.

Grid	Nodes	Cells	Grid shape
grid1	378	672	triangular
grid2	1428	2688	triangular
grid3	4193	4032	quadrilateral
grid4	16449	16128	quadrilateral
grid5	65153	64512	quadrilateral
grid6	259329	258048	quadrilateral
grid7	248215	495432	quadrilateral

the performance metric like Flops, DRAM bytes and run time of the can be computed precisely in this way.

We implement the roofline model to give some performance insights into memory bandwidth and floating-point operations. Roofline [21], [22] is a bound and bottleneck analysis function, it chooses the minimum value of either current peak machine performance, or peak DRAM bandwidth multiply arithmetic intensity, so that it provides insights into the primary factors affecting the performance of computer systems [23].

To measure the workload during the porting process, we apply productivity metric to quantify how efficiently HOUR2D code is developed with different programming models [24], specifically the "code divergence" is the average of the pairwise distances between the applications in different code versions A,

$$D(A) = \binom{|A|}{2}^{-1} \sum d(a_i, a_j), (\{a_i, a_j\} \subset A) \quad (11)$$

in which $d_{a,b}$ originates from the same code in the number of Source Line of Code(SLOC) [25] normalized to the smaller application, the detailed equation is shown in eq. (12).

$$d(a, b) = \frac{|SLOC(a) - SLOC(b)|}{\min(SLOC(a), SLOC(b))} \quad (12)$$

B. Performance Results

We use the complete grids to verify the correctness of output flow field, two intuitive shapes are chosen to display the stable flow field as fig. 5 shows. The subfigure fig. 5a displays the final density of NACA airfoil illustration, the various color refers to differentiated values. While fig. 5b is the pressure of flow around double cylindrical, the flow clusters clusters in front of the first circular and forms relatively high pressure, the reversed side of the circular forms low pressure.

We choose OpenMP-based code as a benchmark to assess the performance of other two languages. Thread scalability is first evaluated with first six computational grids for the convenience of comparison, the run time is displayed in fig. 6, and the number of thread varies from one to twenty. It can be inferred from the figure that the code obtains considerable scalability as the growth rate of the running time is roughly the same as that of the grid size. Besides, twenty-thread parallelization achieves a speedup of 6.0x - 8.1x comparing with serial execution according to different grids, the different speedup of grid may be affected by several reasons like insufficient parallelism for small-scale grid, memory access exacerbation as grid size increases and so on.

The comparisons for three languages is applied after evaluating OpenMP code base, we analyze the speedup based on the serial execution for first six grids as fig. 7 shows. The colored columnars are presented under the same optimization conditions, grid renumbering and mixed precision strategy are not included. The GPU-based code shows relatively lower speedup than OpenMP in small-scale grids, it's due to the fact that the grid data is insufficient in parallelism gain to cover the data movement cost. As the grid size increases, GPU-based code shows priority to OpenMP's, particularly, CUDA is much better than OpenACC owe to the fine-tuning of thread scheduling, better memory hierarchy control, and some memory access optimizations. Generally, OpenACC's

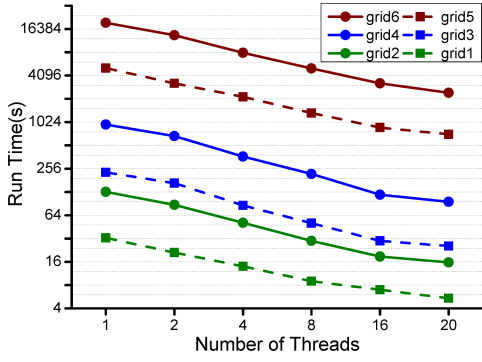


Fig. 6. The run time of OpenMP-based code with six different grid meshes

speedup reaches 75% to 90% of CUDA's, besides, UM approach is enabled in OpenACC-based code. The CUDA, OpenMP, OpenACC based code obtains a maximal speedup of 42.9x, 35.3x, and 8.1x among six grids comparing with serial execution, respectively.

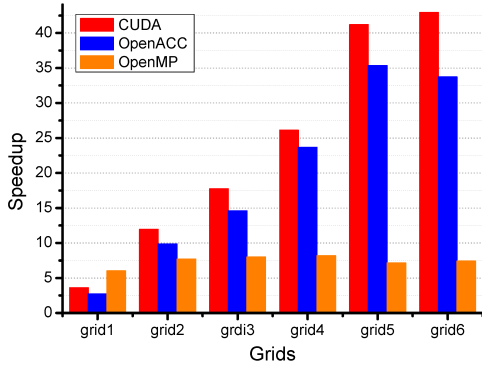


Fig. 7. The speedup of the OpenMP, CUDA, OpenACC based code comparing with serial execution of original code.

To further explore the computing performance, we build the roofline model of all three programming models to find the possible bottleneck with floating-point operations and memory access, the execution details in the CPU are collected by Intel Vtune Profiler, while the Nvidia Nsight Profiler is utilized in GPU. The final chart is shown in fig. 8, the abscissa is the arithmetic intensity which represents the amount of data required (transported from DRAM to cache) for each floating-point operation, and the ordinate is the double-precision floating-point operations achieved per second, besides, the red and blue attributes belong to V100 GPU and Intel Xeon E5 CPU respectively, the solid line is the theoretical limit of the hardware unit, and the scatter points are the measured values through our experiments, moreover, the red dot shows the execution of CUDA-based code while the red star belongs to OpenACC, the different scatter points of the same color display the analysis of different grids.

We can infer from fig. 8 that the HOUR2D executions of all three models are faced with memory access bottleneck even if some memory optimization methods are applied, especially for CUDA-based code when grid size extends,

this may be the increasing deterioration of frequent access to multi-dimensional array for element and cell integral, and the most important, non-consecutive memory access caused by the unstructured grid which is generally acknowledged as a tough issue for HPC researchers in CFD field. What's more, the achieved Flops can be ranked as CUDA ζ OpenACC ζ OpenMP due to the abundant thread concurrency in GPU, particularly for the larger grids.

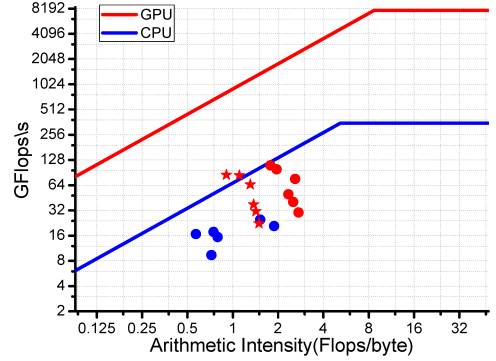


Fig. 8. The illustration of roofline performance model for three programming models

C. Productivity Evaluation

Although the CUDA-based code shows the absolute performance advantage over OpenMP and OpenACC, meanwhile CUDA certainly consumes the most effort on code tuning. So we use quantitative metric detailed in eq. (12) to further evaluate our workload as table IV shows, in which the second column is the porting workload from *desktop* version to current code, and the *desktop* is taken as the benchmark version with 2900 total source lines. The metric $d_{(current,desktop)}$ displays the relative workload porting from the desktop version to the current version as the eq. (10) shows, the fourth and fifth row stands for the situation of whether to use UM method or not, the bigger metric d represents more porting workload and lower productivity. So under the basis of OpenMP-based code, the workload of the CUDA is 8.2 times larger and the OpenACC using UM is 2.7 times larger, however, this quantified number has an underlying assumption that the development difficulty of different programming models keeps consistent.

TABLE IV
PORTABILITY EVALUATIONS WHEN PORTING FROM DESKTOP CODE TO THREE PROGRAMMING MODELS

Current Version	SLOC	$d_{current,desktop}(\%)$
<i>OpenMP</i>	34	1.17
<i>CUDA</i>	280	9.67
<i>OpenACC_{UM}</i>	94	3.24
<i>OpenACC_{nonUM}</i>	161	5.56

The *relative effort time productivity (RDTP)* concept connects the performance and productivity which is

$\Psi_{relative}$ =speedup/relative effort, it's useful under the condition of the same optimization level for three programming models, so the sort through Ψ according to the metric above is: $\Psi_{OpenMP} > \Psi_{CUDA} > \Psi_{OpenACC}$. The OpenMP performs best because of the fairly high productivity, and CUDA is better than OpenACC. It's worth noting that *RDTP* takes performance and productivity equally important which is not always true in reality, striking the appropriate balance between the performance and productivity relies on the ultimate use of the code [26].

V. CONCLUSIONS AND FUTURE WORK

We have presented the migration of a practical high-order DG application named HOUR2D into three programming models running on two architectures, performance analysis, and portability are further evaluated.

We first discuss some optimization methods in the light of data structure and computing format, the grid renumbering approach is used to relieve the discontinuous memory access, then the mixed-precision method to maximize the floating-point operations. We also capture the performance on CPU and GPU platforms with seven grids, concretely the CUDA, OpenMP, and OpenACC based code achieves roughly a speedup of 42.9x, 8.1x, and 35.3x based on the serial execution, then we find the memory access issue by using the roofline model which needs further research, the productivity of different programming models are measured with quantified metric.

We plan to carry out our future work in two aspects. On the one hand, we improve the memory bandwidth and the floating-point efficiency of the high-order algorithm. On the other hand, we evaluate the performance portability of our algorithm in more programming models to offer a practical assessment to the CFD developers.

REFERENCES

- [1] N. Grube, E. Taylor, and P. Martin, "Assessment of weno methods with shock-confining filtering for les of compressible turbulence," in *18th AIAA Computational Fluid Dynamics Conference*, p. 4198, 2007.
- [2] W. H. Reed and T. R. Hill, "Triangular mesh methods for the neutron transport equation," tech. rep., Los Alamos Scientific Lab., N. Mex.(USA), 1973.
- [3] M. Li, W. Liu, L. Zhang, and X. He, "Applications of high order hybrid dg/fv schemes for two-dimensional rans simulations," *Procedia Engineering*, vol. 126, pp. 628–632, 2015. *Frontiers in Fluid Mechanics Research*.
- [4] L. Zhang, L. Wei, H. Lixin, D. Xiaogang, and Z. Hanxin, "A class of hybrid dg/fv methods for conservation laws ii: Two-dimensional cases," *Journal of Computational Physics*, vol. 231, no. 4, pp. 1104–1120, 2012.
- [5] Y. Xia, L. Luo, and H. Luo, "Openacc-based gpu acceleration of a 3-d unstructured discontinuous galerkin method," in *52nd Aerospace Sciences Meeting*, p. 1129, 2014.
- [6] W. Pazner and P.-O. Persson, "Stage-parallel fully implicit rungekutta solvers for discontinuous galerkin fluid simulations," *Journal of Computational Physics*, vol. 335, pp. 700–717, 2017.
- [7] D. Zhijian and X. Gongnan, "Parallel discontinuous galerkin finite element method for computing hyperbolic conservation law on unstructured meshes," *International Journal of Numerical Methods for Heat & Fluid Flow*, vol. 31, 2021.
- [8] M. S. Fabien, M. G. Knepley, R. T. Mills, and B. M. Rivière, "Manycore parallel computing for a hybridizable discontinuous galerkin nested multigrid method," *SIAM Journal on Scientific Computing*, vol. 41, no. 2, pp. C73–C96, 2019.
- [9] M. Kronbichler, N. Fehn, P. Munch, M. Bergbauer, K.-R. Wichmann, C. Geitner, M. Allalen, M. Schulz, and W. A. Wall, "A next-generation discontinuous galerkin fluid dynamics solver with application to high-resolution lung airflow simulations," in *Proceedings of the International Conference for High Performance Computing, Networking, Storage and Analysis, SC '21*, (New York, NY, USA), Association for Computing Machinery, 2021.
- [10] P. L. Roe, "Approximate riemann solvers, parameter vectors, and difference schemes," *Journal of computational physics*, vol. 43, no. 2, pp. 357–372, 1981.
- [11] B. Cockburn and C.-W. Shu, "The runge–kutta discontinuous galerkin method for conservation laws v: multidimensional systems," *Journal of Computational Physics*, vol. 141, no. 2, pp. 199–224, 1998.
- [12] E. Cuthill and J. McKee, "Reducing the bandwidth of sparse symmetric matrices," in *Proceedings of the 1969 24th national conference*, pp. 157–172, 1969.
- [13] D. Burgess and M. B. Giles, "Renumbering unstructured grids to improve the performance of codes on hierarchical memory machines," *Advances in Engineering Software*, vol. 28, no. 3, pp. 189–201, 1997.
- [14] D. A. Patterson, "Latency lags bandwidth," *Communications of the ACM*, vol. 47, no. 10, pp. 71–75, 2004.
- [15] A. Abdelfattah, H. Anzt, E. G. Boman, E. Carson, T. Cojean, J. Dongarra, A. Fox, M. Gates, N. J. Higham, X. S. Li, *et al.*, "A survey of numerical linear algebra methods utilizing mixed-precision arithmetic," *The International Journal of High Performance Computing Applications*, vol. 35, no. 4, pp. 344–369, 2021.
- [16] F. Tisseur, "Newton's method in floating point arithmetic and iterative refinement of generalized eigenvalue problems," *SIAM Journal on Matrix Analysis and Applications*, vol. 22, no. 4, pp. 1038–1057, 2001.
- [17] I. Kampolis, X. Trompoukis, V. Asouti, and K. Giannakoglou, "Cfd-based analysis and two-level aerodynamic optimization on graphics processing units," *Computer Methods in Applied Mechanics and Engineering*, vol. 199, no. 9–12, pp. 712–722, 2010.
- [18] P. Gomes, T. D. Economon, and R. Palacios, "Sustainable high-performance optimizations in su2," in *AIAA Scitech 2021 Forum*, p. 0855, 2021.
- [19] W. Li, G. Jin, X. Cui, and S. See, "An evaluation of unified memory technology on nvidia gpus," in *2015 15th IEEE/ACM international symposium on cluster, cloud and grid computing*, pp. 1092–1098, IEEE, 2015.
- [20] Y. Che, L. Zhang, Y. Wang, C. Xu, W. Liu, and Z. Wang, "Microarchitectural performance comparison of intel knights corner and intel sandy bridge with cfd applications," *The Journal of Supercomputing*, vol. 70, no. 1, pp. 321–348, 2014.
- [21] S. Williams, A. Waterman, and D. Patterson, "Roofline: an insightful visual performance model for multicore architectures," *Communications of the ACM*, vol. 52, no. 4, pp. 65–76, 2009.
- [22] M. Harris, "Mapping computational concepts to gpus," in *ACM SIGGRAPH 2005 Courses*, pp. 50–es, 2005.
- [23] E. D. Lazowska, J. Zahorjan, G. S. Graham, and K. C. Sevcik, *Quantitative system performance: computer system analysis using queueing network models*. Prentice-Hall, Inc., 1984.
- [24] S. L. Harrell, J. Kitson, R. Bird, S. J. Pennycook, J. Sewall, D. Jacobsen, D. N. Asanza, A. Hsu, H. C. Carrillo, H. Kim, *et al.*, "Effective performance portability," in *2018 IEEE/ACM International Workshop on Performance, Portability and Productivity in HPC (P3HPC)*, pp. 24–36, IEEE, 2018.
- [25] V. Nguyen, S. Deeds-Rubin, T. Tan, and B. Boehm, "A sloc counting standard," in *Cocomo ii forum*, vol. 2007, pp. 1–16, Citeseer, 2007.
- [26] J. , M. Oivo, and A. Jedlitschka, "Software productivity and effort estimation," *Journal of Software: Evolution and Process*, vol. 27, no. 7, pp. 465–466, 2015.